Available online at www.sciencedirect.com
SCIENCE DIRECT®
Coordination Chemistry Reviews 249 (2005) 1423–1433
COORDINATION CHEMISTRY REVIEWS
www.elsevier.com/locate/ccr

Luminescence in complexes with Au(I)–Tl(I) interactions

E.J. Fernández[a], A. Laguna[b,*], J.M. López-de-Luzuriaga[a]

[a] *Departamento de Química, Universidad de La Rioja, Grupo de Síntesis Química de La Rioja, U.A.-CSIC. Madre de Dios 51, E-26006 Logroño, Spain*
[b] *Departamento de Química Inorgánica, Instituto de Ciencia de Materiales de Aragón, Universidad de Zaragoza-CSIC, E-50009 Zaragoza, Spain*

Received 16 June 2004; accepted 30 July 2004
Available online 21 September 2004

Contents

Abstract

Following three different strategies gold–thallium complexes are prepared. One of them consists of the use of bidentate bridging ligands, the second one uses the acid–base process, and the third uses a gold metallocryptand, which is able to encapsulate a thallium atom. The structures of these complexes show discrete molecules, extended linear chains or two- or three-dimensional networks, all of them displaying luminescence. The emission is strongly dependent on the structures and, thus, extended linear chains are luminescent in solid state, while discrete molecules are also luminescent in solution. Ab initio calculations allow us to establish the energy of the Au–Tl interaction. density functional theory (DFT) and time dependent-density functional theory (TD–DFT) calculations allow us to predict the excitations that lead to emission of radiation for the different type of complexes. From these it is concluded that metal–metal interactions, as well as atom environments, are the main aspects that affect the energy of the emissions.

Keywords: Gold; Thallium; Metal–metal interactions; Luminescence; Theoretical calculations

1. Introduction

As has been well established, relativistic heavy atoms have a marked tendency to form aggregates with metal–metal distances shorter than the sum of their van der Waals radii. Particularly abundant is the case of gold(I) containing complexes which tend to form dimers, oligomers or even uni- or multidimensional polymers based on gold(I)–gold(I) interactions (van der Waals radii of gold(I) = 1.66 Å [1]) of a strength comparable to hydrogen bonds [2]. This structural situation was initially pointed out by Schmidbaur in the 1980s [3] and encouraged experimental chemists to carry out an exhaustive search of structural information and the theorists to construct theoretical models to compare with the experimental data. Thanks to these efforts, it is nowadays generally accepted that these interactions arise from correlation and relativistic effects that are of particular importance in the case of gold, although relativistic effects are a minor component of the interaction energy stabiliza-

* Corresponding author. Tel.: +34 976 1185; fax: +34 976 1187.
E-mail address: alaguna@unizar.es (A. Laguna).

0010-8545/$ – see front matter © 2004 Elsevier B.V. All rights reserved.
doi:10.1016/j.ccr.2004.07.010

tion. Nevertheless, the great availability and development of X-ray diffraction analyses has allowed us to show that gold(I) is not an exception in the periodic table and that other metal atoms with closed-shell configurations can display the same phenomenon. Thus, examples of interactions between centres with d^{10}–d^{10} (Ag(I)–Ag(I) [4], Cu(I)–Cu(I) [5], Hg(II)–Hg(II) [6], Pt(0)–Pt(0) [7], Pd(0)–Pd(0) [8]), d^8–d^8 (Pt(II)–Pt(II) [9]), and s^2–s^2 (Tl(I)–Tl(I) [10], Pb(II)–Pb(II) [11]) configurations, or even between centres of different configurations such as s^2–d^8 (Tl(I)–Pt(II) [12], Tl(I)–Pd(II) [13], Tl(I)–Ir(I) [14]), s^2–d^{10} (Tl(I)–Au(I) [15], Pb(II)–Au(I) [16]) and d^8–d^{10} (Pt(II)–Au(I) [17], Pt(II)–Hg(II) [18], Pt(II)–Ag(I) [19], Pd(II)–Au(I) [20]) have been reported and theoretical studies of selected examples have been carried out [21]. From these studies it has been shown that Au(I) and Tl(I) represent the two extremes of the *metallophilicity* and, thus, while aurophilic attractions can be considered the upper extreme of the metallophilic attractions with values up to 46 kJ mol^{-1}, interactions involving Tl(I) centres appear as the weakest ones, even below 20 kJ mol^{-1} [22]. The theoretical explanation of these values is that while aurophilic attractions are enhanced by the relativistic effects, these weaken the van der Waals attractions between the s^2 metal atoms [23]. Taking into account these comments, it seems that the study of the interaction between Au(I) and Tl(I) centres is of particular interest since this appears between centres in oxidation state +1 and these centres would normally be expected to repel each other. In contrast, some products containing both metal centres at distances shorter than the sum of their van der Waals radii (3.62 Å) [1] are surprisingly stable, with an additional electrostatic force in some or possible packing forces or the ligand architecture in others as responsible for this fact (see below). For instance, as noted in this review, metallophilicity between gold(I) and thallium(I) centres in extended linear chain compounds with an average metal–metal separation of 3.03 Å is estimated at about 276 kJ mol^{-1}, of which 80% consists of an ionic interaction [24]. Consequently, the rationalization of the bonding in these species still remains as a challenge for synthetic and theoretical chemists.

In addition to the curious nature of this interaction from a theoretical viewpoint, it can be considered responsible for very important physical properties of the materials that contain it, for example the luminescence. The special nature of the emissive properties makes the complexes suitable for use as sensors for volatile organic or inorganic compounds [25]. Of course, the thorough study on such aspects as metal–metal distances, environments around the metal centres and donor characteristics of the ligands attached to them may lead to knowledge of the conditions needed for tuneability of the emissive properties in these derivatives. Thus, for instance, thallium(I) displays in these complexes an astonishing complexity in coordination number and geometry [26], which may also imply that vacant coordination sites are available for interacting with a wide variety of substrates. In addition, many of them possess a very intense and long-lived luminescence with emission energies spanning a wide range in the visible spectrum. All these characteristics render this class of complexes perfect candidates for the fabrication of LEDs or different luminescent sensors. In short, understanding the photophysics and photochemistry of these materials could permit the judicious design of complexes chosen for individual applications whose demand in the microelectronic industry or medicine is increasing every day.

The objective of this paper is not only to review the gold–thallium luminescent complexes, but also to show a very promising area of research that, in spite of the relatively small number of complexes prepared to date, have led to the first steps of a new class of luminescent materials with promising uses for practical applications.

2. Different approaches in the design of luminescent Au(I)–Tl(I) complexes displaying metal–metal interactions

Complexes displaying gold–thallium interactions can be prepared following three basic strategies:

(a) The first consists of the use of bridging ligands containing different donor centres, which permits a selective coordination of these atoms to both metals, placing them at distances shorter than the sum of their van der Waals radii. This strategy produces supported gold–thallium interactions.
(b) The second one produces unsupported gold–thallium interactions through reactions between basic gold(I) complexes and acid thallium(I) salts giving rise to supramolecular networks via acid–base stacking.
(c) Finally, the third strategy also leads to unsupported gold–thallium interactions by encapsulation of a thallium centre in a dinuclear gold(I) cryptand.

2.1. Bridged gold–thallium interaction

In 1988 Fackler et al. reported the first extended heterobimetallic linear chain that exhibits luminescence [15,16]. The [AuTl(MTP)$_2$] complex (MTP = μ-$CH_2P(S)Ph_2$) is formed by reacting Tl_2SO_4 with PPN[Au(MTP)$_2$], which contains a linear two-coordinate Au(I) centre. In this heteronuclear complex the gold(I) atom is coordinated to two ylide carbon atoms and the thallium centre to two sulfur atoms of the ligands, forming a double bridge between the metal centres. The gold–thallium distance in this unit is 2.959(2) Å. This molecule forms a one-dimensional polymer along one crystallographic axis of the lattice with nearly equal Tl–Au spacings (intermolecular 3.003(2) Å) (Fig. 1).

The luminescence of this complex in solid state shows both the emission and the bandwidth temperature dependence. Thus, the emission at 565 nm (halfwidth = 2140 cm^{-1}) at 298 K is shifted to red (602 nm (HW = 1550 cm^{-1})) when the temperature is decreased to 77 K. In contrast, the complex is not luminescent in solution at 298 K recovering this

property on freezing at 77 K (536 nm). This last result is interpreted in terms of a bigger aggregation of $[AuTl(MTP)_2]$ units in solid state. The lifetime of 0.98 μs after laser excitation at 355 nm and the large separation between excitation and emission peaks indicate that the emission process in this complex is phosphorescence.

2.2. Unsupported gold–thallium interactions built by the acid–base process

In the early 1990 a thorough study of the luminescence properties of a gold–thallium network was done by Patterson and co-workers [27]. The complex studied was $Tl[Au(CN)_2]$ [28], prepared by reaction of $TlNO_3$ and $K[Au(CN)_2]\cdot 2H_2O$. In this case the structural data show two thallium–gold interactions of 3.474 and 3.491 Å, with the rest of Au–Tl distances being longer than 3.62 Å, corresponding to the sum of their van der Waals radii.

The complex shows a very important dependence of both the emission and the lifetime on temperature. Thus, while two bands of different intensity (at 575 and 518 nm) appear at 5 K, at 300 K, the former, assigned to luminescent traps, disappears and the most energetic one shifts to the blue when increasing the temperature. Thus, shifts to 509 at 40 K and to 483 nm at 360 K are observed. The dependence of the lifetime on the temperature is even more pronounced, changing from 176 μs at 1.7 K to about 50 ns at 400 K. The lowering of the absorption and luminescence energies compared to the related and previously reported $Cs[Au(CN)_2]$ [28b] permitted Patterson to conclude that the gold–thallium interactions present in this compound are the factor that affects the energies, intensities and rates of deactivation of the various states involved in the absorption and luminescence processes.

On the other hand, the reaction between the basic $[Au(C_6F_5)_2]^-$ anion and the acid Tl^+ cation in the presence of two equivalents of triphenylphosphine oxide (Eq. (1)) leads to a complex of stoichiometry $[AuTl(C_6F_5)_2(OPPh_3)_2]$, which is the first extended unsupported gold–thallium linear chain [29].

$$2OPPh_3 + TlNO_3 + Li[Au(C_6F_5)_2] \rightarrow [AuTl(C_6F_5)_2(OPPh_3)_2] \quad (1)$$

This chain displays gold–thallium interactions of 3.0358(8) and 3.0862(8) Å and the environment around the thallium centre is distorted trigonal-bipyramidal, taking into account the stereochemically active inert pair of this atom. This complex is luminescent in the solid state at room temperature (494 nm) and at 77K (494 and 530 nm) but it is not luminescent in acetone solution, recovering the optical properties when the solvent is evaporated. Interestingly, when the process of dissolution is carried out in a halogenated solvent and it is irradiated with UV light the luminescence is quenched and the evaporation of the solvent gives rise to a luminescent uncharacterised grey solid. Nevertheless, if it is not irradiated, the original complex is recovered without any change. These facts allowed us to conclude, first, that the emission arises from interactions between the metals, second, that the gold–thallium interactions are broken in dilute solutions and, finally, third, that the excited state reached by UV-radiation is able to react with halocarbons in an electron transfer reaction, making, perhaps, this product appropriate as an irreversible sensor for halocarbons (Fig. 2).

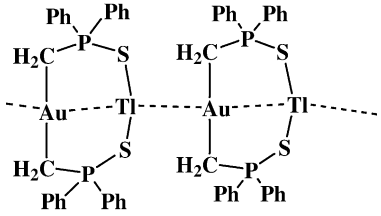

Fig. 1. The repeat structure of $[AuTl(MTP)_2]$ showing inter- and intramolecular gold–thallium interactions.

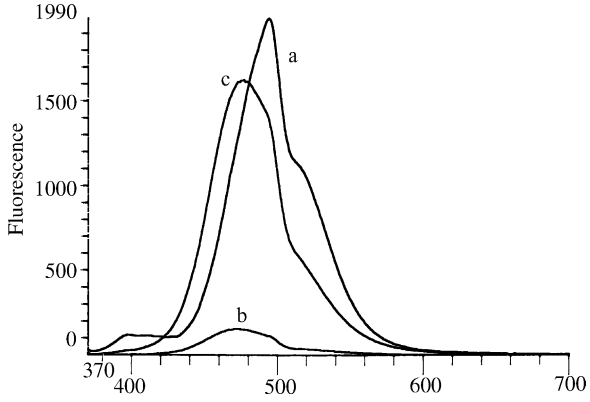

Fig. 2. Luminescence of $[AuTl(C_6F_5)_2(OPPh_3)_2]_n$: (a) in solid state; (b) in dichloromethane; (c) after evaporation of dichloromethane. *Y*-axis: fluorescence in arbitrary units; *X*-axis: wavelength in nm.

When the starting gold precursor is $[Au(C_6Cl_5)_2]^-$ the same reaction with the thallium salt and triphenylphosphine oxide in tetrahydrofuran or acetone leads to products of stoichiometry $[Tl(OPPh_3)][Tl(OPPh_3)L][Au(C_6Cl_5)_2]_2$ [24], whose structures display also extended linear chains with alternating metal centers in a zig-zag disposition with Au–Tl distances of 3.0529(3), 3.14528(3), 3.1630(3) and 3.3205(3) Å (L: tetrahydrofuran) or 3.2438(3), 3.0937(3), 3.2705(4) and 3.1492(3) Å (L: acetone). Interestingly, in these cases the environments around the thallium atoms are alternatively pseudotetrahedral and distorted trigonal-bipyramidal (Fig. 3).

The luminescence in these complexes is also temperature dependent and shows a site-selective excitation in the solid state at low temperature. In contrast, in solution both complexes lose their optical properties. In the case of the complex with tetrahydrofuran two emissions appear at 510 (exc. 412) and 461 nm (exc. 329 nm) and, in the acetone derivative, at 526 (exc. 408) and 465 nm (exc. 334 nm). The fact that in both complexes the pairs of excitation and emissions appear at similar energies allows one to conclude that the

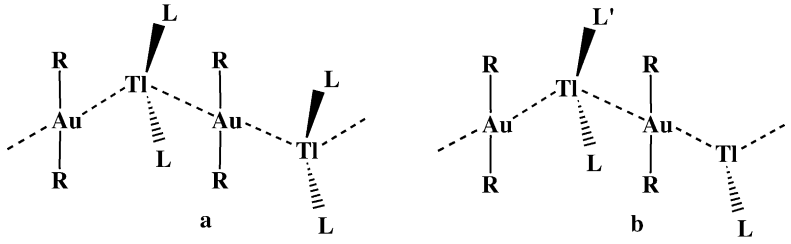

Fig. 3. Linear chains showing different environments at the thallium centres. (a) L: $OPPh_3$, R: C_6F_5; (b) L: $OPPh_3$, L′: acetone or tetrahydrofuran, R: C_6Cl_5.

coordinating solvents do not influence significantly the excited states from which the emissions are produced. It seems likely that both bands are related to the different environments at the thallium centres as confirmed by a theoretical analysis of selected models (see point 3): the gold–thallium interactions with the thallium centre in a tetrahedral environment are responsible for the low energy bands, while the higher energy bands have their origin mainly in the gold–thallium interactions in which the thallium atom possesses a distorted trigonal-bipyramidal disposition.

In the same manner, the only difference in the aryl groups bonded to gold produces important changes in the solid state structures formed in similar acid–base reactions in the presence of 4,4′-bipyridine [30]. Thus, the reaction of the basic $[AuR_2]^-$ (R = C_6F_5, C_6Cl_5) with the salt $TlPF_6$ in the presence of 4,4′-bipyridine in tetrahydrofuran leads to highly luminescent materials of stoichiometry $[Tl(bipy)]_2[Au(C_6F_5)_2]_2$ or $[Tl(bipy)][Tl(bipy)_{0.5}(thf)][Au(C_6Cl_5)_2]$ (bipy: 4,4′-bipyridine), respectively. The X-ray diffraction analyses shows, as before, metal–metal distances shorter than the sum of their van der Waals radii as well as complexes consisting of planar polymers formed by repetition of Tl–Au–Au–Tl (a) or Tl–Au–Tl′–Au (b) moieties, respectively (see Fig. 4), linked through bidentate bridging bipy ligands. While in the former the layers are associated via Tl···F contacts between different planes, in the latter two polymeric layers are linked through additional bridging bipy molecules.

Very interestingly and different to that occurring in other gold thallium chains, in the complex $[Tl(bipy)]_2[Au(C_6F_5)_2]_2$ (Fig. 4a), the tetramer unit found presents a nonalternating sequence of ions [+ − − +], which is clearly at variance with the simple rules of Coulomb forces.

As before, both materials display a strong fluorescence in solid state at room temperature and at 77 K but not in solution, indicating that the interactions among the metal centres are responsible for the emissions. Nevertheless, the dependence of the temperature in both species is different and, thus, while the pentachlorophenyl derivative (Fig. 4b) shows the usual shift to the red (from 620 to 642 nm) when decreasing the temperature, in the case of the pentafluorophenyl complex the shift is to higher energies (from 525 to 507 nm). This fact is likely to be related to the different metal arrangements in both complexes and analysed through time

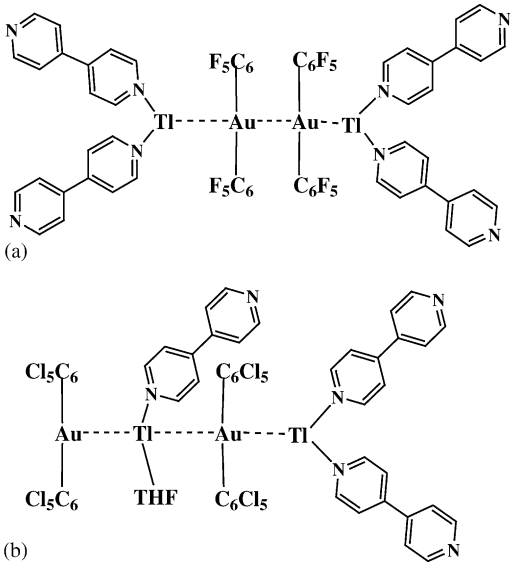

Fig. 4. Tl–Au–Au–Tl (a) and Au–Tl–Au–Tl′ (b) disposition of metal atoms $[Tl(bipy)]_2[Au(C_6F_5)_2]_2$ and $[Tl(bipy)][Tl(bipy)_{0.5}(thf)][Au(C_6Cl_5)_2]$.

dependent-density functional theory (TD–DFT) calculations (see below).

An extension of this work was the attempt to prepare extended linear chains using the perhalophenyl strategy but in the absence of ligands that could affect the atom environments, which, as we have seen, greatly affects the luminescence. This led to recognition of the other essential factor in the synthesis of unsupported gold–thallium complexes: the solvent used in the process, which affects the final structure and, hence, the optical properties of the derivatives. Thus, for instance, the reaction between $NBu_4[Au(C_6Cl_5)_2]$ and $TlPF_6$ in acetone leads to the synthesis of a product of stoichiometry $[Au_2Tl_2(C_6Cl_5)_4]$·acetone [31]; while if the solvent is tetrahydrofuran the stoichiometry of the product is $[AuTl(C_6Cl_5)_2]_n$ [25a].

The crystal structure of the complex $[Au_2Tl_2(C_6Cl_5)_4]$·acetone consists of a tetranuclear unit where the metals are held together through four unsupported Au–Tl interactions within the range 3.0331(6)–3.1887(6) Å and an additional Tl–Tl interaction of 3.6027(6) Å, resulting in a loosely bound butterfly cluster (Fig. 5).

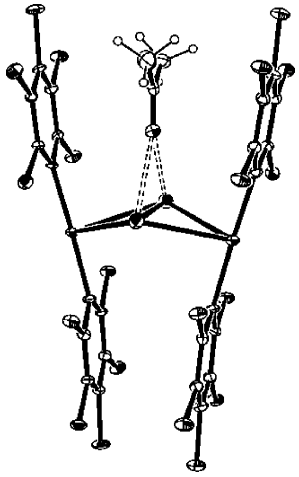

Fig. 5. Crystal structure of $[Au_2Tl_2(C_6Cl_5)_4]$·acetone showing the butterfly disposition of the metals.

This complex is luminescent in the solid state at room temperature (exc. at 400 nm, em. at 556 nm) and at 77 K (exc. at 420, em. at 556 nm) showing an interesting independence of the temperature which is likely to be due to the environmental rigidity (*luminescence rigidochromism*). This not fully understood phenomenon, is assigned to a substantial dependence of the emission maxima on the environmental rigidity and has been described in other luminescent gold-heteropolynuclear systems [16,30,32]. In addition and very interestingly, this complex is also luminescent in solution showing a solvent dependence. For instance, acetone, tetrahydrofuran and acetonitrile solutions of this complex show emission bands at 566 (exc. at 356), 528 (exc. at 358) and 539 nm (exc. at 346 nm), respectively, values that are close in energy to the emission observed in the solid state, which could be indicative of the same excited state in both states, solution and solid state. Conductivity measurements of this complex in solution are characteristic of a 2:1 electrolyte. Therefore, both this result and the unusual luminescent properties in solution can be in agreement with the existence of a Tl(I)–Tl(I) interaction in solution which is stabilized by solvent molecules with donor capabilities (Eq. (2)). Simple $TlPF_6$ salt does not show these solvent-stabilized luminescent properties in solution being this behaviour specific to Au_2Tl_2 butterfly compound.

$$[Au_2Tl_2(C_6Cl_5)_4] \cdot (CH_3)_2C{=}O \xrightarrow{\text{solvent}} [Tl_2(\text{solvent})_n]^{2+} + 2[Au(C_6Cl_5)_2]^- \quad (2)$$

On the other hand, as we commented previously, the same reaction carried out in tetrahydrofuran leads to a product of stoichiometry $[AuTl(C_6Cl_5)_2]_n$. In this case the product consists of a 1-D linear polymer chain parallel to the crystallographic *z*-axis with unsupported Au–Tl interactions of 3.0044(5) and 2.9726(5) Å and a Au–Tl–Au angle of 180.0° (Fig. 6a). Each Tl atom has eight long contacts with the chlorine atoms of its own chain and from adjacent ones. This situation may contribute to the stability of the system and, in addition, makes holes parallels to the *z*-axis as large as 10.471 Å to appear (Fig. 6b).

The solid shows a strong luminescence in the solid state at room temperature and at 77 K, but not in solution, where the interactions between the metal centres no longer exist, a fact, as we previously commented, common to the rest of the extended systems. Interestingly, the emission at room temperature has a dependence on the particle size, which is interpreted in terms of a certain degree of semiconductivity in the complex. In fact, SEM images taken of the solid without coating with a conductor appear clear, suggesting that the material is not an insulator.

On the other hand, perhaps the most striking characteristic of this material is the ability to change its colour and luminescence properties when the solid is exposed to a variety of organic vapours, for instance, acetone, acetonitrile, triethylamine, acetylacetone, tetrahydrothiophene, 2-fluoropyridine, tetrahydrofuran or pyridine. In addition, the colour changes back to that of the starting material upon heating to 100 °C over a period that requires from a few seconds, for acetone, to 10 min, for pyridine, which adds another important characteristic to this system, the reversibility, which can make it appropriate for practical applications.

Exposure of this material at room temperature and pressure of the vapours mentioned also produces a shift in the

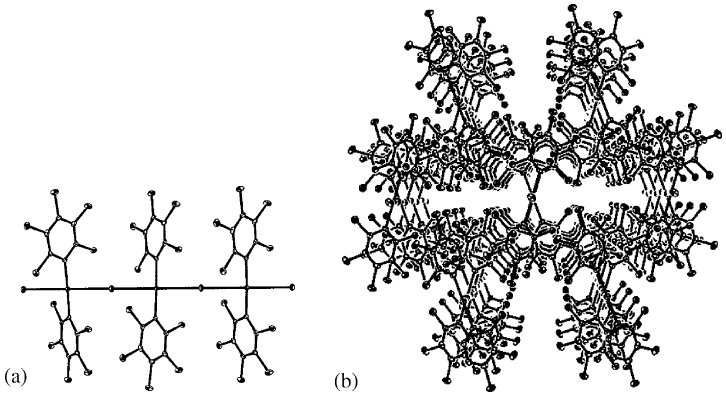

Fig. 6. Crystal structure of $[AuTl(C_6Cl_5)_2]_n$ (a) and packing viewed down the crystallographic *z*-axis (b). The tunnels have diameters between 3.23 and 10.42 Å.

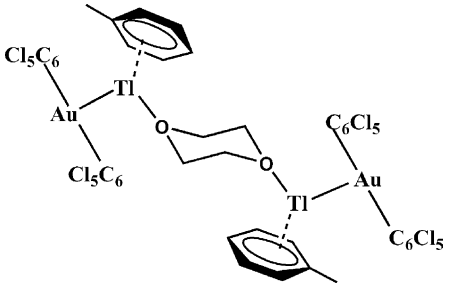

Fig. 7. Drawing of the structure of [{AuTl(C_6Cl_5)$_2$(toluene)}$_2$(dioxane)].

emission maximum of the starting material. Thus, the emission band changes from 531 to 507 (THF), 511 (NEt_3), 513 (NCMe), 532 (Me_2CO), 567 (THT), 627 (2-Fpy), 646 (py) or 650 nm (acetylacetone), in addition, all of them shift to the red when the measurements are carried out at 77 K. Of course, the interaction between the organic molecules and the unsaturated thallium atoms affects the gold–thallium distances, which are responsible for the emission. These results together with the recent analysis of the UV–vis absorption and infrared spectra, crystal and powder X-ray diffraction analysis, thermogravimetric methods etc. of this material, which are compared to the products obtained in the reactions of $[AuTl(C_6Cl_5)_2]_n$ and the ligands in solution, has allowed us to obtain a close approximation to the molecules that are formed in the process of absorption of vapours by this complex [25b].

A very striking complex can be obtained from $[AuTl(C_6Cl_5)_2]_n$ in its reaction with dioxane in a 2:1 molar ratio, in toluene [33]. The product has a stoichiometry [{AuTl(C_6Cl_5)$_2$(toluene)}$_2$(dioxane)] and the structure consists of a tetranuclear unit containing two $[AuC_6Cl_5)_2]^-$ units, two Tl^+ centres and a dioxane molecule linked via unsupported Au–Tl and Tl–O interactions with a toluene molecule interacting with each thallium centre in a η^6-mode (Fig. 7).

This complex shows an unprecedented Au–Tl distance of only 2.8935(3) Å, shorter than the sum of their covalent radii (2.92 Å [1]), and an η^6-like π-arene contact with the thallium centres resulting in a nearly trigonal planar environment (355.2°) for these atoms. Significantly, the stereoactivity of the inert pair, which is stereochemically active in the rest of the complexes, is not apparent in this case. This fact points out doubts regarding the nature of the Au–Tl interaction.

The luminescence in this complex seems to be related to such a special interaction and structure and, thus, the usual characteristics observed for other Au–Tl systems do not appear in this complex. Thus, for instance, in spite of exhibiting the shortest Au–Tl distance ever reported, the product emits in the blue region at room temperature (442 nm) and at 77 K (468 nm), and is not luminescent in solution. In accord with the previous comments for the other systems, a reduction in the metal–metal distance should lead to a reduction in the band gap energy and a red shift of the emission. Consequently, this product should show the least energetic emission reported for these systems. In addition, its long lifetime (double exponential decay of 1844 and 752 ns) is indicative of a phosphorescent process, similar to that noted for $[Au_2Tl_2(C_6Cl_5)_4]$·acetone, also a discrete molecule, but different to what occurs in extended linear chains, which showed shorter lifetimes indicating, perhaps, fluorescence.

On the other hand, in addition to the surprising vapochromic characteristics of the complex $[AuTl(C_6Cl_5)_2]_n$, and thanks to the coordinative unsaturation of the thallium atoms, this complex and the homologous $[AuTl(C_6F_5)_2]_n$ can behave as starting materials in reactions, not only with neutral ligands, but also with metal complexes. As before, variation of the aryl groups bonded to gold lead to different structures that have a strong influence in their optical properties. As a first entry in reactions with metal complexes we chose Tl(acac) as starting product. The reactions between the heteronuclear gold–thallium complex and Tl(acac) in a 1:1 or 1:2 molar ratio leads to complexes of stoichiometry $[AuTl_2(acac)(C_6Cl_5)_2]$ and $[AuTl_3(acac)_2(C_6F_5)_2]$, respectively [34]. Both structures display gold–thallium and thallium–thallium interactions (see Fig. 8), which are considered to be responsible for their optical behaviour.

Thus, for instance, in the solid state both complexes show a single emission at room temperature at 531 and 429 nm, respectively, which is indicative of a different origin, while at 77 K they display two independent emissions with two different excitation profiles at 463 and 588 nm for $[AuTl_2(acac)(C_6Cl_5)_2]$ and at 427 and 507 nm for $[AuTl_3(acac)_2(C_6F_5)_2]$. The behaviour of these complexes in solution is different to that of other chains and both complexes are luminescent in acetonitrile showing a single emission in the blue region at 380 and 390 nm, respectively. The analyses of these data and comparison of those with the luminescence properties of the starting material Tl(acac) in solution or in solid state allow us to assign the less energetic bands as arising from electronic excited states coming from the d^{10}(Au)–s^2(Tl) interactions, while the bands appearing at higher energies are likely due to the presence of $Tl_2(acac)_2$ units that remain even in solution. As in the case of the butterfly complex $[Au_2Tl_2(C_6Cl_5)_4]$·acetone, it seems that the presence or absence of thallium–thallium interactions is essential in the luminescence of these materials in solution.

Also following the acid–base strategy Fackler and Burini and co-workers have recently reported a series of sandwich derivatives by interaction of π-base trinuclear gold(I) complexes of the type $[Au(\mu\text{-}C^2,N^3\text{-bzim})]_3$ (bzim: 1-benzylimidazolate) and $[Au(\mu\text{-}C(OMe)=NCH_3)]_3$ with the acid cation Tl^+, to give $[Tl\{[Au(\mu\text{-}N^3,C^2\text{-bzim})]_3\}_2]^+$ or $[Tl\{[Au(\mu\text{-}C(OEt)=NC_6H_4CH_3)]_3\}_2]PF_6$, containing $[Au_3TlAu_3]$ units (Fig. 9), whose polymerisation through gold–gold interactions leads to infinite chains [35].

The thallium ion centre is bonded to six gold atoms to form a distorted trigonal prism, with gold–thallium distances from 2.9711(7) to 3.0448(7) Å in $[Tl\{[Au(\mu\text{-}N^3,C^2\text{-bzim})]_3\}_2]^+$ and from 3.0673(4) to 3.1075(4) Å in $[Tl\{[Au(\mu\text{-}C(OEt)=NC_6H_4CH_3)]_3\}_2]PF_6$. In addition, there

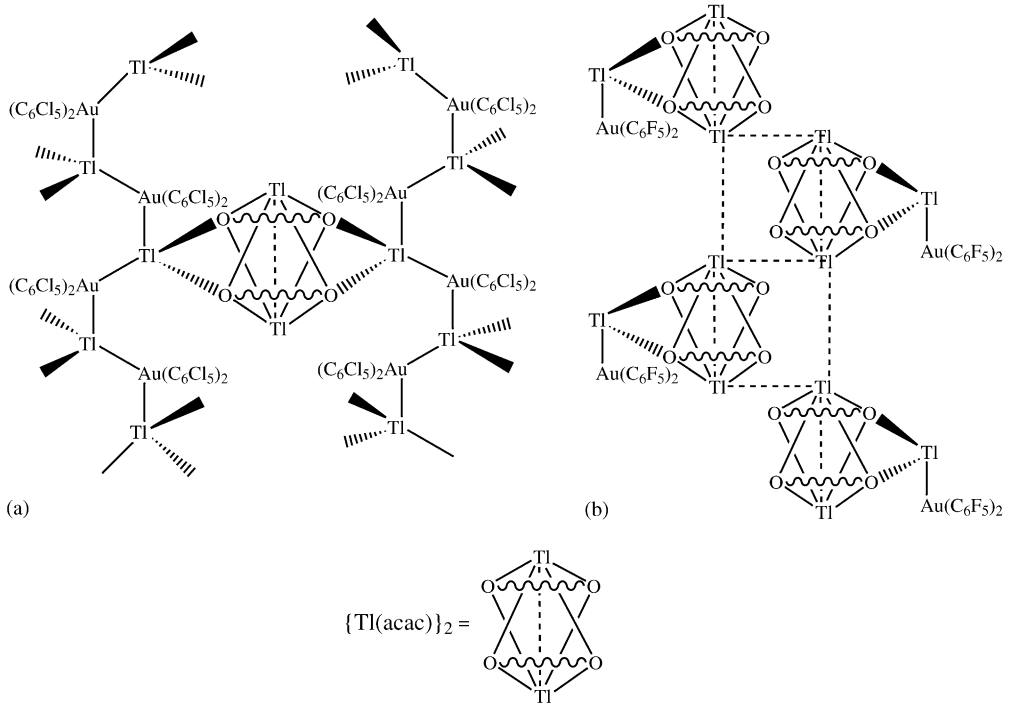

Fig. 8. Drawings of the structures of $[AuTl_2(acac)(C_6Cl_5)_2]$ (a) and $[AuTl_3(acac)_2(C_6F_5)_2]$ (b).

are gold–gold interactions between two close sandwich units in a range from 3.0525(4) to 3.1089(7) Å in both complexes.

The emission spectra of these compounds display low energy phosphorescence; they also exhibit luminescence thermochromism with red shifts in the emission maxima when cooling the crystals to 77 K. These luminescence bands are associated with excited states delocalised along the crystallographic axis of the chain. Thermal contraction lead to a reduction in the intermolecular metal–metal distances along the chain and reduce the band gap energy. Interestingly, luminescence of the complex $[Tl\{[Au(\mu\text{-}N^3,C^2\text{-bzim})]_3\}_2]^+$ is also dependent on the excitation wavelength: at 77 K a strong green emission is observed upon excitation with 420 nm, whereas a yellow emission is seen upon excitation with 475 nm. This behaviour indicates the presence of two electronically uncoupled luminescent sites.

2.3. Unsupported gold–thallium interactions built by encapsulation in a gold(I) cryptand

Catalano and co-workers have recently shown an interesting alternative to the commented strategies. It consists of the use of a new class of metallocryptands with a cavity created by linking two three-coordinate Au(I) fragments with three diphosphanylphenanthrolines molecules acting as bridges between them. The thallium centre is encapsulated between both gold atoms appearing to be unsupported metal–metal closed-shell interactions. Thus, employing the ligand 2,9-bis-(diphenylphosphino)-1,10-phenanthroline (P_2phen) they have synthesised a dinuclear gold(I) cryptand, which is able to selectively host a Tl(I) ion (Fig. 10) [36].

The gold–thallium interactions are very short (2.9171(5) and 2.9109(5) Å) displaying an almost linear arrangement

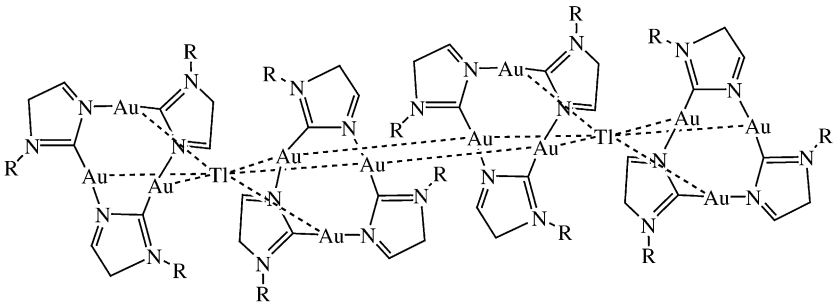

Fig. 9. Drawing of the structure of $[Tl\{[Au(\mu\text{-}N^3,C^2\text{-bzim})]_3\}_2]^+$.

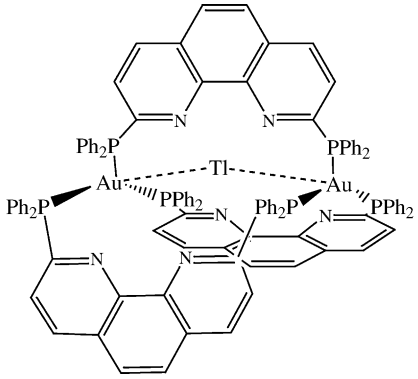

Fig. 10. Drawing of the structure of $[Au_2Tl(P_2phen)_3]^{3+}$.

(Au–Tl–Au angle of 174.47(2) Å). This derivative is strongly luminescent at 600 nm, in solution and the solid state showing an additional less intense band at 390 nm. The low energy emission can be assigned to metal-centred (Au–Tl) phosphorescence based on its large Stoke's shift, long lifetime (10 μs in solution increasing in solid state up to 220 μs) and solvent independence. By contrast, the high energy band has a much shorter lifetime (10 ns) and is assigned to a fluorescence process.

3. Theoretical analyses of the optical properties

The first contribution to the explanation of the nature of the bonding in gold–thallium complexes and, hence, to the origin of the optical properties observed came also with the first synthesis from Fackler's laboratory in 1989 in the complex $[AuTl(MTP)_2]$ [15,16]. The molecular orbital calculations were made by the Fenske–Hall method and they indicated that although the interactions between both metallic fragments cannot be considered as a formal-metal bond, there is significant overlap of the 6s orbital of gold with the $6p_z$ orbital of thallium and between the $6p_z$ orbital of gold with the 6s of thallium (Fig. 11).

In accord with view, the HOMO is an antibonding orbital mainly of thallium, while the LUMO is a bonding orbital with contributions from both metal centres. Thus, the HOMO (σ* orbital) is formed by mixing filled and empty atomic levels, a

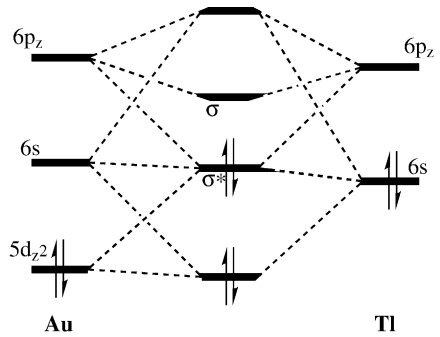

Fig. 11. Qualitative molecular orbital diagram for the Au–Tl interaction.

process that is associated with relativistic effects on the electrons in these heavy metal atoms, while, the excitation from the HOMO to the LUMO orbitals would produce a formal metal–metal bond in the excited state. The big structural difference between both states should give rise to a big Stokes shift, as observed in this complex, but, as we commented, it is not a general rule and several other factors must be considered.

Another contribution to this study, using extended Hückel type calculations, came from Patterson's laboratory and deals with the electronic structure and the nature of the Au–Tl interaction in the complex $Tl[Au(CN)_2]$ [27].

Thus, a first result is that relativistic effects play an important role in the Tl–Au interactions by influencing the relative 6s and 6p orbital energies of Tl and Au. The second important conclusion obtained in this study is that at a Au–Tl separation of 3.0 Å, the HOMO–LUMO gap is smaller than that for the isolated $[Au(CN)_2]^-$ ion. The Au–Tl interaction is considered to be responsible for the lowering of the absorption and luminescence energies in this complex if compared to the isostructural $Cs[Au(CN)_2]$ and also influences the rates of deactivation. In fact, the interaction of the thallium atom with the gold centre is considered to be responsible for the lack of the fluorescence process observed in the cesium complex thanks to a more rapid singlet–triplet interconversion [27].

The next contribution to these studies came from our laboratory using ab initio calculations at HF and MP2 levels of theory. As a first step, we studied the nature of the Au(I)–Tl(I) interaction on the simplified model system $[Tl(OPH_3)_2][Au(C_6H_5)_2]$ [24]. Density functional theory (DFT) and TD–DFT calculations allowed us to predict the excitations that lead to emission of radiation for the different type of complexes.

Thus, regarding the ab initio calculations on the Au–Tl interactions, these were done with non relativistic and relativistic effective core potentials. The comparison of both levels allowed us to evaluate the relativistic effects in the Au–Tl metallophilic attraction, this being ca. 21%. In addition, the comparison between QR-HF and MP2-QR levels gave rise to an interaction energy of 275 kJ mol^{-1}, consisting of 80% of ionic interaction and 20% of van der Waals interaction at a equilibrium distance of 3.02 Å.

On the other hand, the interesting luminescence behaviour of the perhalophenyl-gold–thallium complexes was studied by DFT and TD–DFT calculations. The former allows us to study the electronic structure of those compounds and a population analyses to check the contribution of each atom to each occupied orbital. The TD–DFT calculations allow us to predict theoretical excitations that can be compared in energy and intensity with the experimental ones, as well as the transitions between orbitals involved in each excitation.

Thus, for instance, in the case of the extended linear chain complex $[AuTl(C_6Cl_5)_2]_n$ [25a], whose structure displays a perfect linear environment for the metal centres, the model $((C_6Cl_5)_2Au\cdots Tl\cdots(C_6Cl_5)_2Au\cdots Tl)$ for the DFT

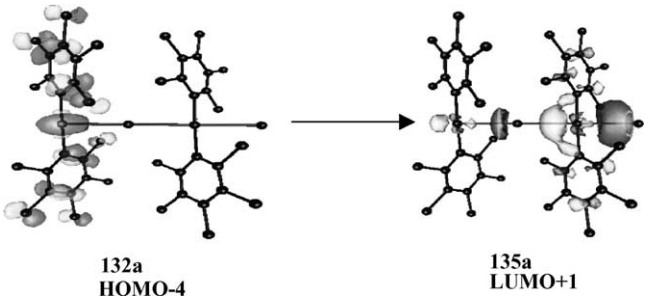

Fig. 12. Orbitals involved in the main contribution to the excitation maximum (calc.499 nm, exp. 490 nm).

calculations was obtained for X-ray diffraction results and the analyses of the highest occupied orbitals shows that they are mainly centred in the $[Au(C_6Cl_5)_2]^-$ units. In contrast, the shape of the unoccupied ones shows that they are located mainly on the metal atoms with a high participation of thallium. The TD–DFT calculations lead to the singlet excitation energies of the model and the analyses of the more intense theoretical excitations indicates electron transfer between different parts and atoms of the metallic chain, which is in accordance with a excited state delocalised along the chain (Fig. 12), as we commented previously.

The supramolecular structures found in the solid state as well as the metal environments also influence the excited states responsible for the light emission. For instance, in the case of the previously noted complexes $[Tl(bipy)]_2[Au(C_6F_5)_2]_2$ and $[Tl(bipy)][Tl(bipy)_{0.5}(thf)][Au(C_6Cl_5)_2]$ (bipy: 4,4′-bipyridine) [30], the DFT analyses match the experimental result and shows that in both models the highest occupied orbitals are mainly centred on carbon atoms with important contribution of gold and thallium in selected excitations, this contribution increasing when the energy of the excitations increases. The calculations also indicate that only a few orbitals are of appropriate symmetry and energy for intense transitions, being the theoretical excitations with higher oscillator strengths those involving mostly metal-based orbitals. Therefore, as is experimentally proposed, the luminescence of these complexes involves mainly orbitals of the metals. The different distribution of the metals in the complexes strongly affects their luminescence characteristics, but in both cases the origin of the transitions seems to be located in the anionic $[AuX_2]^-$ parts of the molecule and the arrival on the thallium centres. In addition, the shape of the orbitals have a $d_z{}^2\sigma^*$ character on gold and a $6p\sigma^*$ on thallium, therefore, the transitions between these antibonding orbitals would not produce a bond order enhancement and only a small structural distortion in the excited state is expected, in accordance with the fluorescence processes experimentally observed.

The different environments of these atoms also affect the luminescence in these complexes. For instance, in the case of $[Tl(OPPh_3)][Tl(OPPh_3)L][Au(C_6Cl_5)_2]_2$ (L: acetone or tetrahydrofuran) [24], as we commented previously, the emissions are likely to come from two different electronic states that can be related to the two coordination environments of the thallium centres, tetrahedral and trigonal-bipyramidal. In this case the DFT and TD–DFT calculations also offer a reasonable explanation of the optical properties observed. The analyses were carried out by means of four models obtained from the X-ray crystal structure determination, in accordance with the four different Au–Tl distances found; two of them containing the thallium in a tetrahedral environment and the other two in a trigonal-bipyramidal one (Fig. 13).

As can be seen in both models, two groups of excitations appear, even though the Au–Tl distances in the second are quite different. As before, the origin of most of the transitions is located in the $[Au(C_6H_5)_2]^-$ part of the model and the arrival orbitals are mostly thallium based, which leads to transitions with a Au–Tl charge transfer character. Nevertheless, a careful inspection of the excitation energies reveals that in the case of the tetrahedral thallium the less energetic excitations (420–440 nm) appear at lower energies if compared with the corresponding zone for the trigonal-bipyramidal (370–410 nm). In contrast, the high energy zone is more populated with excitations due to the trigonal-bipyramidal thallium atoms. Therefore, these calculations offer an explanation for the experimental site-selective excitation, which is considered to be due to the presence of different environments around the thallium(I) centres. These facts have shown that the thallium environments are even more

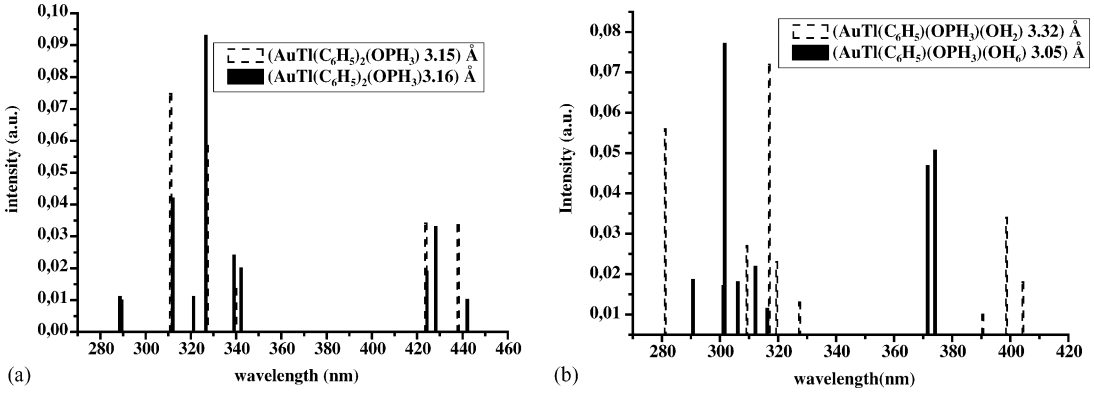

Fig. 13. Theoretical electronic spectra for the tetrahedral (a) and distorted trigonal-bipyramidal (b) models.

important than the metal–metal distances in determining the optical properties. Finally, the comparison of these results with that obtained for the model $[Tl(OPPH_3)_2][Au(C_6H_5)_2]$ $[Tl(OPPH_3)_2][Au(C_6H_5)_2]$[24] allows us to observe an increasing metal-based character of the orbitals responsible for the luminescence when the nuclearity of the model system increases.

In accordance with the unconventional luminescent behaviour of the complex $[Au_2Tl_2(C_6Cl_5)_4]$·acetone [31], which shows a butterfly disposition of the metal centres, the TD–DFT calculations offer a surprising result. Thus, while the origin of the luminescent transitions is in both $[Au(C_6H_5)_2]^-$ fragments, the orbital from which the emission is produced is completely based on both thallium atoms, which retrain an interaction in the solid state and is proposed to remain in solution. In this case, the excited state shows an orbital formed by both thallium atoms with a similar contribution (see Fig. 14) instead of contributing in different proportion to the emissive state as seen in previous models. This fact could be in accordance with the different energy found in the experimental emission as well as with the luminescence observed in solution, where the break-up of the thallium–thallium interaction is, apparently, not produced.

Finally, in the case of the complex $[\{AuTl(C_6Cl_5)_2$ (toluene)$\}_2$(dioxane)] [33], which shows an unprecedented structure and luminescence, the DFT and TD–DFT calculations do not permit us to unequivocally assign the short gold–thallium distance (2.8935(3) Å) as the origin of the luminescence. In fact, as noted above, previous Fenske–Hall molecular orbital calculations indicated that a reduced Au–Tl distance would produce a better overlap of the $5d_z^2$ and 6s orbitals, reducing the energy of the emission. The TD–DFT calculations show the $[Au(C_6Cl_5)_2]^-$ units as the origin of the electronic transitions and the thallium centres as the emitter atoms, similarly to other systems previously described. In contrast, in this case, the energy of the emission is the highest one reported in these Au–Tl systems. This result which is probably related to the special nature of the gold–thallium interaction probably needs higher levels of calculation.

A conclusion of this short review is that acid–base reactions open a new promising and exciting area that permits the synthesis of complexes with unsupported metal–metal interactions, interesting from both a synthetic and theoretical point of view. In addition, the interesting optical properties of some of the complexes could make them promising candidates for practical applications. Future variations of ligands and metals and theoretical studies could be useful to assign the excited states that are responsible for the light emissions as well as to know the nature of the metal–metal interactions.

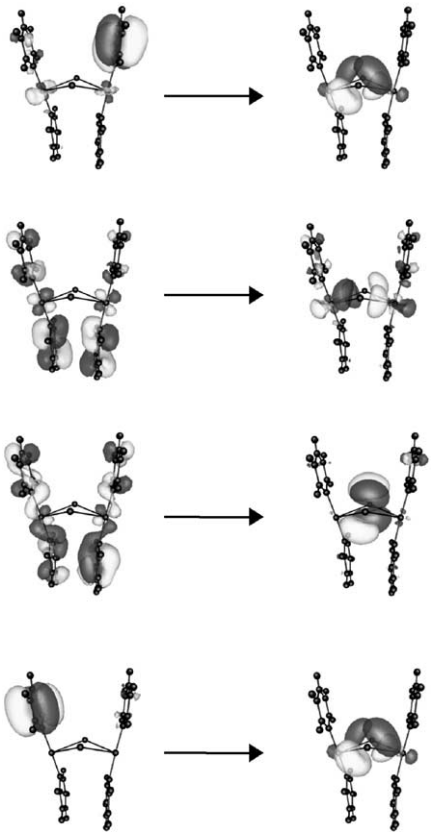

Fig. 14. TD–DFT singlet excitation calculations for the $[Au_2Tl_2(C_6H_5)_4]$ model system at the energies 356.9, 358.1, 360.9 and 361.3 nm (from above to below). Notice the antibonding character of the unoccupied orbitals.

Acknowledgements

The D.G.I. (MCYT)/FEDER (BQU2001-2409), the CAR (ANGI2001/28) are thanked for financial support.

References

[1] http://www.webelements.com.
[2] H. Schmidbaur, Gold Bull. 33 (2000) 3.
[3] (a) F. Scherbaum, A. Grömann, B. Huber, C. Krüger, H. Schmidbaur, Angew. Chem. Int. Ed. Engl. 27 (1988) 1544;
(b) F. Scherbaum, A. Grömann, G. Müller, H. Schmidbaur, Angew. Chem. Int. Ed. Engl. 28 (1989) 463;
(c) H. Schmidbaur, F. Scherbaum, B. Hubert, G. Müller, Angew. Chem. Int. Ed. Engl. 27 (1988) 419.
[4] See for example;
(a) H.H. Karsch, U. Schubert, Z. Naturforsch. 37b (186) (1982);
(b) T. Tsuda, S. Ohba, M. Takahashi, M. Ito, Acta Crystallogr. C 45 (1989) 887;
(c) M. Jansen, Angew Chem. Int. Ed. Engl. 26 (1987) 1098.
[5] See for example;
A. Heine, R. Herbst-Irmer, D. Stalke, J. Chem. Soc. Chem. Commun. 1729 (1993).
[6] See for example;
H. Schmidbaur, H.-J. Öller, D.L. Wilkinson, B. Huber, G. Müller, Chem. Ber. 122 (1989) 31.
[7] See for example;
S. Otsuka, J. Organomet. Chem. 200 (1980) 191.
[8] Y.-L. Pan, J.T. Mage, M.J. Fink, J. Am. Chem. Soc. 115 (1993) 3842.
[9] See for example;
(a) T. Tanase, Y. Kudo, M. Ohno, K. Kobayashi, Y. Yamamoto, Nature 344 (1990) 526;

(b) N.M. Boag, M. Green, J.A.K. Howard, F.G.A. Stone, H. Wadepohl, J. Chem. Soc., Dalton Trans. (1981) 862.
[10] See for example;
(a) R. Blom, H. Werner, J. Wolf, J. Organomet. Chem. 354 (1988) 293;
(b) H. Pritzkow, P. Jennische, Acta Chem. Scan. A 29 (1975) 60;
(c) B. Krebs, H. Greiwing, Z. Anorg. All. Chem. 616 (1992) 145.
[11] See for example;
L.A. Bengtsson, R. Hoffmann, J. Am. Chem. Soc. 115 (1993) 2666.
[12] See for example;
J.K. Nagle, A.L. Balch, M.M. Olmstead, J. Am Chem. Soc. 110 (1988) 319.
[13] A.L. Balch, B.J. Davis, E.Y. Fung, M.M. Olmstead, Inorg. Chim. Acta 212 (1993) 149.
[14] A.L. Balch, J.K. Nagle, M.M. Olmstead, P.E. Reedy Jr., J. Am. Chem. Soc. 109 (1987) 4123.
[15] See for example;
S. Wang, J.P. Fackler Jr., C. King, J.C. Wang, J. Am. Chem. Soc. 110 (1988) 3308.
[16] S. Wang, G. Garzón, C. King, J.C. Wang, J.P. Fackler Jr., Inorg. Chem. 28 (1989) 4623.
[17] See for example;
J.C. Jeffery, P.A. Jelliss, F.G.A. Stone, Inorg. Chem. 32 (1993) 3943.
[18] T.F. Carlson, J.P. Fackler Jr., R.J. Staples, R.E.P. Winpenny, Inorg. Chem. 34 (1995) 426.
[19] H.-K. Yip, H.-M. Lin, Y. Wang, C.-M. Che, J. Chem. Soc., Dalton Trans. (1993) 2939.
[20] O. Crespo, A. Laguna, E.J. Fernández, J.M. López-de-Luzuriaga, P.G. Jones, M. Teichert, M. Monge, P. Pyykkö, N. Runeberg, M. Schütz, H.-J. Werner, Inorg. Chem. 39 (2000) 4786.
[21] P. Pyykkö, Chem. Rev. 97 (1997) 597.
[22] (a) P. Schwerdtfeger, Inorg. Chem. 30 (1991) 64;
(b) G. Treboux, J.C. Barthelat, J. Am. Chem. Soc. 115 (1993) 4870;
(c) C. Janiak, R. Hoffmann, J. Am. Chem. Soc. 112 (1990) 5024.
[23] P. Pyykkö, M. Straka, T. Tamm, Phys. Chem. Chem. Phys. 1 (1999) 3441.
[24] E.J. Fernández, A. Laguna, J.M. López-de-Luzuriaga, F. Mendizábal, M. Monge, E. Olmos, J. Pérez, Chem. Eur. J. 9 (2003) 456.
[25] (a) E.J. Fernández, J.M. López-de-Luzuriaga, M. Monge, M.E. Olmos, J. Pérez, A. Laguna, A.A. Mohamed, J.P. Fackler Jr., J. Am. Chem. Soc. 125 (2003) 2022;
(b) E.J. Fernández, J.M. López-de-Luzuriaga, M. Monge, M. Montiel, M.E. Olmos, J. Pérez, A. Laguna, F. Mendizábal, A.A. Mohamed, J.P. Fackler Jr., Inorg. Chem. 43 (2004) 3573.
[26] F. Weisbrock, H. Schmidbaur, and references therein, J. Am. Chem. Soc. 125 (2003) 3622.
[27] Z. Assefa, F. DeStefano, M.A. Garepapaghi, J.H. LaCasce Jr., S. Oulette, M.R. Corson, J.K. Nagle, H.H. Patterson, Inorg. Chem. 28 (1991) 2868.
[28] (a) P. Fischer, J. Mesot, B. Lucas, A. Ludi, H. Patterson, A. Hewat, Inorg. Chem. 36 (1997) 2791;
(b) N. Blom, A. Ludi, H.B. Bürgi, K. Tichy, Acta Cristallogr. C 40 (1984) 1767.
[29] O. Crespo, E.J. Fernández, P.G. Jones, A. Laguna, J.M. López-de-Luzuriaga, A. Mendía, M. Monge, E. Olmos, Chem. Commun. (1998) 2233.
[30] E.J. Fernández, P.G. Jones, A. Laguna, J.M. López-de-Luzuriaga, M. Monge, M.E. Olmos, J. Pérez, Inorg. Chem. 41 (2002) 1056.
[31] E.J. Fernández, J.M. López-de-Luzuriaga, M. Monge, M.E. Olmos, J. Pérez, A. Laguna, J. Am. Chem. Soc. 124 (2002) 5942.
[32] (a) M. Wrighton, D.L. Morse, J. Am. Chem. Soc. 96 (1974) 998;
(b) M.K. Itokazu, A.S. Polo, N.Y. Murakami Iha, J. Photochem. Photobiol. A Chem. 160 (2003) 27.
[33] E.J. Fernández, A. Laguna, J.M. López-de-Luzuriaga, M.E. Olmos, J. Pérez, Chem. Commun. (2003) 1760.
[34] E.J. Fernández, A. Laguna, J.M. López-de-Luzuriaga, M. Monge, M. Montiel, M.E. Olmos, J. Pérez, Organometallics 23 (2004) 774.
[35] A. Burini, R. Bravi, J.P. Fackler Jr., R. Galassi, T.A. Grant, M.A. Omary, B.R. Pietroni, R.J. Staples, Inorg. Chem. 39 (2000) 3158.
[36] V.J. Catalano, B.L. Bennett, H.M. Kar, J. Am. Chem. Soc. 121 (1999) 10235.